Reaction of a Carbon Equivalent of Iodosylbenzene with Iron–Porphyrins: A Ready Access to *N*-Alkylporphyrin Complexes Involving Five-Membered Fe–O–C–C–N Metallocycles

Jean-Paul Battioni,[†] **Isabelle Artaud,**[†] **Daniel Dupré,**[†] **Philippe Leduc,**[†] **Irèna Akhrem,**[†1]
Daniel Mansuy,*[†] **Jean Fischer,**[‡] **Raymond Weiss,***[‡] **and Irène Morgenstern-Badarau**[§]

Contribution from the Laboratoire de Chimie et de Biochimie Pharmacologiques et Toxicologiques, U. A. 400, Université René Descartes, 75270 Paris, Cedex 06, France, Laboratoire de Cristallochimie, ERA 08, Université Louis Pasteur, 67070 Strasbourg Cedex, France, and Laboratoire de Spectrochimie des Eléments de Transition, ERA 672, Université de Paris-Sud, 91405 Orsay Cedex, France. Received January 28, 1986

Abstract: Iron(II)–porphyrin complexes, $Fe^{II}P$ (P = tetraarylporphyrin: TPP, TpClPP, and TTP), react with the iodonium ylide C_6H_5I=X (X = $CC(O)CH_2C(CH_3)_2CH_2C(O)$) to give Fe^{II}–bis-*N*-alkylporphyrin complexes exhibiting a structure in which the metal and two trans pyrrole nitrogen atoms are bound respectively to the oxygen and the carbon atom of two X moieties. The bismetallocyclic structures of these Fe^{II} high-spin complexes result from the insertion of two –O–C–C– groups of the X moiety into two trans Fe–N bonds. These structures deduced from X-ray crystallography for one complex and proposed from the others agree with their elemental analysis and ^1H NMR, UV-vis, and mass spectra. In contrast, complexes Fe^{III}(P = tetraarylporphyrin = TPP, TpClPP, TTP, and TMP)(ClO_4) react with the iodonium ylide C_6H_5I=X to give the corresponding high-spin monometallocyclic Fe^{III}-*N*-alkylporphyrin complexes whose structures have been deduced from (i) their elemental analysis, (ii) their mass and ^1H NMR spectra, and (iii) the complete transformation of three of them (TPP, TpClPP, and TTP) into the corresponding bismetallocyclic Fe^{II}–bis-*N*-alkylporphyrin complexes upon reaction of their one-electron reduction products with the iodonium ylide. The corresponding monometallocyclic Fe^{II}-*N*-alkylTMP complex fails to react with C_6H_5I=X under identical conditions probably because of the greater hindrance of the TMP derivative. The formation and physical properties of this new class of iron-*N*-alkylporphyrin complexes involving five-membered Fe–O–C–C–N metallocycles are discussed in relation to the complexes formed during the suicidal inactivation of cytochrome P-450 by terminal monosubstituted 1-alkenes.

High-valent Fe^{IV}– or Fe^V–oxo[2,3] complexes have been prepared by the reaction of iron–porphyrins with potential oxygen atom donors. They are believed to be the active species involved in alkane hydroxylation and alkene epoxidation by iodosylbenzene catalyzed by cytochrome P-450[4] or iron porphyrins.[5] Their nitrogen analogues, the Fe^{IV}– or Fe^V–imido (or iron(II)– or iron(III)–nitrene) complexes, seem to be formed upon oxidation of 1,1-dialkylhydrazines by cytochrome P-450.[6] Porphyrin–iron–nitrene complexes, Fe^{IV}=N—NR$_2$ ↔ Fe^{II}←N—NR$_2$, prepared by oxidation of such hydrazines, have been completely characterized.[7] Such iron–nitrene complexes might be involved

in the transfer of *N*-tosyl moiety of the nitrogen analogue of PhIO, PhI=N—tosyl, into aliphatic C–H bonds[8] or double bond of alkenes,[9] catalyzed by iron(III)–porphyrins.

Their carbon analogues, the iron–carbene complexes, seem to be formed upon oxidation of certain compounds by cytochrome P-450,[10] and several porphyrin–iron–carbene complexes have now been prepared and characterized.[11] The reactions of the carbon analogues of PhIO, the iodonium ylides, PhI=CRR′, with iron–porphyrins are therefore of interest.

$$Fe=O \qquad Fe=N—R \qquad Fe=CRR'$$

$$PhI=O \qquad PhI=N—R \qquad PhI=CRR'$$

The results described therein show that, depending upon the reaction conditions, such a iodonium ylide, compound 1 (CRR′ = $CC(O)CH_2C(CH_3)_2CH_2C(O)$ = X), reacts with iron–porphyrins to give either *N*-alkylporphyrin complexes involving one five-membered Fe–O–C–C–N metallocycle or bis-*N*-alkylporphyrin–iron(II) complexes involving two Fe–O–C–C–N me-

†Université René Descartes.
‡Université Louis Pasteur.
§Université de Paris-Sud.
(1) Present address: Institute of Organo-Elements Compounds, Academy of Sciences, Moscow, U.S.S.R.
(2) (a) Chin, D. H.; La Mar, G. N.; Balch, A. L. *J. Am. Chem. Soc.* **1980**, *102*, 5945-5947. (b) Chin, D-H.; Balch, A. L.; La Mar, G. N. *J. Am. Chem. Soc.* **1980**, *102*, 1446-1448. (c) Balch, A. L.; Chan, Y. W.; Cheng, R. J.; La Mar, G. N.; Latos-Grazynski, L.; Renner, M. W. *J. Am. Chem. Soc.* **1984**, *106*, 7779-7785. (d) Balch, A. L.; Latos-Granzynski, L.; Renner, M. W. *J. Am. Chem. Soc.* **1985**, *107*, 2983-2985. (e) Groves, J. T.; Takahashi, T. *J. Am. Chem. Soc.* **1983**, *105*, 2073-2074. (f) Schappacher, M.; Weiss, R.; Montiel-Montoya, R.; Trautwein, A.; Tabard, A. *J. Am. Chem. Soc.* **1985**, *107*, 3736-3738.
(3) Groves, J. T.; Haushalter, R. C.; Nakamura, M.; Nemo, T. E.; Evans, B. J. *J. Am. Chem. Soc.* **1981**, *103*, 2884-2885.
(4) (a) Ullrich, V. *Top. Curr. Chem.* **1979**, *83*, 67-104. (b) White, R. E.; Coon, M. J. *Annu. Rev. Biochem.* **1982**, *49*, 315-356.
(5) (a) Groves, J. T.; Nemo, T. E. *J. Am. Chem. Soc.* **1983**, *105*, 5786-5791. (b) Groves, J. T.; Nemo, T. E. *J. Am. Chem. Soc.* **1983**, *105*, 6243-6248. (c) Lindsay-Smith, J. R.; Sleath, P. R. *J. Chem. Soc., Perkin Trans. 2*, **1982**, 1009-1015. Colmann, J. P.; Kodakek, T.; Raybuck, S. A.; Brauman, J. I.; Papazian, L. M. *J. Am. Chem. Soc.* **1985**, *107*, 4343-4345. (e) Traylor, P. S.; Dolphin, D.; Traylor, T. G. *J. Chem. Soc., Chem. Commun.* **1984**, 279-280. (f) Mansuy, D.; Leclaire, J.; Fontecave, M.; Dansette, P. *Tetrahedron* **1984**, *40*, 2847-2857 and references cited therein.
(6) Hines, R. N.; Prough, A. J. *J. Pharmacol. Exp. Ther.* **1980**, *214*, 80-86.

(7) (a) Mansuy, D.; Battioni, P.; Mahy, J. P. *J. Am. Chem. Soc.* **1982**, *104*, 4487-4489. (b) Mahy, J. P.; Battioni, P.; Mansuy, D.; Fischer, J.; Weiss, R.; Mispelter, J.; Morgenstern-Badarau, I.; Gans, P. *J. Am. Chem. Soc.* **1984**, *106*, 1699-1707.
(8) (a) Breslow, R.; Gellman, S. H. *J. Chem. Soc., Chem. Commun.* **1982**, 1400-1401. (b) Breslow, R.; Gellman, S. H. *J. Am. Chem. Soc.* **1983**, *105*, 6728-6729.
(9) Mansuy, D.; Mahy, J. P.; Dureault, A.; Bedi, G.; Battioni, P. *J. Chem. Soc., Chem. Commun.* **1984**, 1161-1163.
(10) (a) Ullrich, V. *Biological Reactive Intermediates*; Jollow, D. J.; Koscis, J. J.; Synder, R.; Vaino, H., Eds.; Plenum Press: New York, 1977; pp 65-82. (b) Mansuy, D.; Battioni, J. P.; Chottard, J. C.; Ullrich, V. *J. Am. Chem. Soc.* **1979**, *101*, 3971-3973.
(11) (a) Mansuy, D. *Pure Appl. Chem.* **1980**, *52*, 681-690. (b) Battioni, J. P.; Chottard, J. P.; Mansuy, D. *Inorg. Chem.* **1982**, *21*, 2056-2062. (b) Battioni, J. P.; Dupre, D.; Guerin, P.; Mansuy, D. *J. Organomet. Chem.* **1984**, *265*, 53-64.

Table I. UV–vis, Mass Spectrometry and Electrochemical Characteristics of Complexes of Type 3 and 5

complex	UV–vis[a]					$E_{1/2}$[b] Fe^{III}/Fe^{II} (mV)	mass spectra[c] m/e (rel intnsty %)		
	λ (nM)		ε (mM^{-1}·cm^{-1})						
3a	454	524	580	655	736	−205		806	668
	(84)	(18)	(8.7)	(4)	(4.9)			(50)	(100)
3b	457	524	578	652	726	−103		942	804
	(104)	(22)	(11)	(5.6)	(6.4)			(100)	(62)
3c	458	526	581	654	736	−174		864	724
	(83)	(18)	(9.6)	(5.4)	(4.9)			(82)	(100)
3d	448	518	574	638	696	−300	1009	975	836
	(71.4)	(12.5)	(7.5)	(3.6)	(sh)		(3)	(100)	(18)
5a	464	562	615	746		+410	944	806	668
	(114)	(10.9)	(16.4)	(4.4)			(100)	(30)	(25)
5b	467	562	620	750		+540	1080	942	804
	(110)	(12.3)	(20)	(5.1)			(98)	(84)	(100)
5c	466	562	622	754		+340	1000	864	724
	(116)	(9.9)	(17.7)	(5.2)			(100)	(55)	(82)

[a] In C_6H_6. [b] Vs. saturated calomel electrode; for complexes 3 in deaerated DMF, 0.2 M LiCl; for complexes 5 in CH_3CN, 0.2 M $LiClO_4$. [c] For complexes 3: M^+, M^+ − Cl, M^+ − Cl − X; for complexes 5 M^+, M^+ − X, M^+ − 2X.

Scheme I

a   P = TPP
b   P = TpClPP
c   P = TTP
d   P = TMP
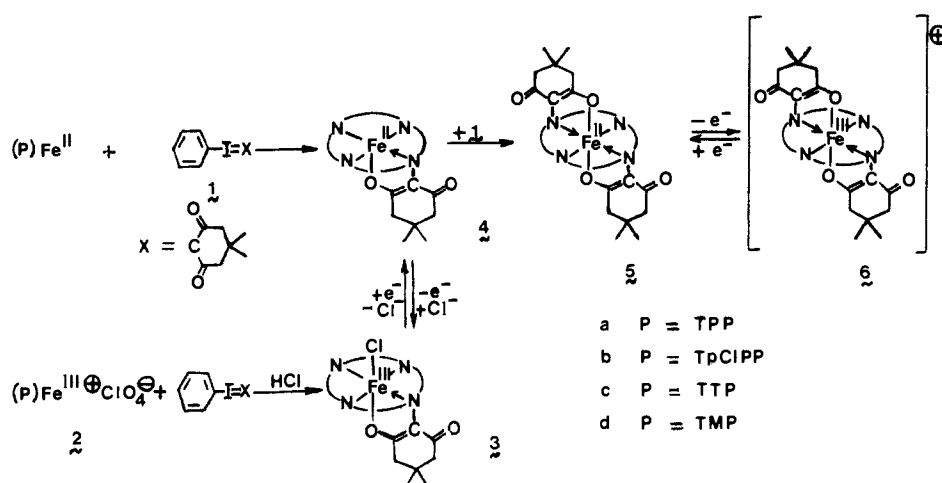
tallocycles. The structures and physicochemical properties of these complexes have been deduced from various spectroscopic methods including an X-ray analysis for one of them.[12] These results definitively establish the existence of their Fe–O–C–C–N metallocycles which derive formally from the insertion of a O–C–C moiety of 1 into iron–nitrogen bonds of the starting iron–porphyrin complexes.

The formation and properties of this new class of iron–*N*-alkylporphyrin complexes are discussed in relation to the complexes formed during the suicidal inactivation of cytochrome P-450 by terminal monosubstituted 1-alkenes.

Results

I. Reaction of C_6H_5I=X, 1, with Iron(II)–Porphyrins. Upon addition under argon of a CH_2Cl_2 solution of $Fe^{II}(TPP)$[13] to a 20-fold excess of the iodonium ylide,[14] C_6H_5I=X (1), the red color of the porphyrin rapidly turned green, and a new complex characterized by a Soret band at 462 nm was formed quantitatively within 0.5 h at 50 °C. After purification by column chromatography and crystallization from CH_2Cl_2–pentane, complex 5a was obtained as a green powder with an almost quantitative yield (>95%).

Identical reactions were performed with $Fe^{II}(TpClPP)$[13] or $Fe^{II}(TTP)$[13] and led to the corresponding complexes 5b and 5c.

(12) A preliminary report on one of these complexes has appeared: Mansuy, D.; Battioni, J. P.; Akhrem, I.; Dupre, D.; Fischer, J.; Weiss, R.; Morgenstern-Badarau, I. *J. Am. Chem. Soc.* **1984**, *106*, 6112–6114.

(13) TPP, TpClPP, TTP, and TMP are respectively used for the dianion of mesotetraphenyl-, mesotetra(parachlorophenyl), mesotetra(4-methylphenyl)-, mesotetra(2,4,6-trimethylphenyl)porphyrin, PPIXDME and DPIXDME for those of proto- and deuterioporphyrin IX dimethylester.

(14) Karele, B.; Neilands, O. *Zh. Org. Khim.* **1968**, *4*, 1818–1822.

However, the reaction of $Fe^{II}(TMP)$[13] with 1 failed to give a similar complex of type 5 (vide infra, part II). See Scheme I.

Characteristics of Complexes 5. In mass spectrometry, all complexes 5 exhibit molecular peaks corresponding to Fe(porphyrin)X_2 and fragments corresponding to the successive loss of one and two X moieties and indicating that the iron–porphyrin ring remains intact after these fragmentations (Table I). Accordingly, the elemental analyses (C, H, N) of complexes 5 correspond to the formula Fe(porphyrin)$(C_8H_{10}O_2)_2$·2H_2O, indicating the formal incorporation of two X moieties into the Fe^{II}–porphyrin complexes and a residual solvation by two water molecules (see Experimental Section).

X-ray Analysis of Complex 5a. Crystals of complex 5a suitable for an X-ray structure determination were obtained by slow crystallization from a CH_2Cl_2–pentane solvent mixture.

The asymmetric unit of the crystals contains two independent half-molecules of bis N-alkylated iron(II) porphyrin which are located on an inversion center and hence presents at least 1̄ symmetry. Table II gives the atomic positional parameters for all non-hydrogen atoms. Figure 1 shows one of these centrosymmetric molecular units together with the labeling scheme used. Table III gives selected bond distances and angles and their mean values.

Complex 5a (Figure 1) presents an unusual bismetallocyclic structure in which two opposite pyrrole nitrogens are alkylated by two X groups. These groups are further ligated axially to iron by one oxygen atom. The two alkylated pyrrole nitrogens, the two porphyrinato nitrogens, and the metal are necessarily coplanar. Whereas the mean value of the two Fe–Np bond distances is 2.082 (5) Å, the Fe–N(alkyl) average bond is 2.242 (5) Å. The axial Fe–O average bond distance is 1.998 (5) Å.

In all the mono-N-alkylated porphyrin complexes whose structures are known so far,[15] the metal–N(alkyl) bond distances

Table II. Atomic Positional Parameters for All Non-Hydrogen Atoms for Complex 5a[a]

atom	x	y	z	B (Å²)
Fe1	0.000	0.000	0.000	2.75 (4)
N1	0.0270 (4)	−0.0936 (4)	0.1255 (5)	3.0 (2)
C11	−0.0530 (6)	−0.1337 (5)	0.1463 (6)	3.2 (2)
C12	−0.0099 (6)	−0.1827 (6)	0.2510 (7)	4.2 (2)
C13	0.0948 (7)	−0.1711 (6)	0.2955 (7)	4.1 (2)
C14	0.1192 (6)	−0.1157 (5)	0.2171 (6)	3.2 (2)
C5	0.2232 (6)	−0.0946 (5)	0.2245 (6)	3.2 (2)
N2	0.1640 (4)	0.0343 (4)	0.0925 (5)	2.8 (2)
C21	0.2420 (6)	−0.0394 (5)	0.1506 (6)	3.0 (2)
C22	0.3369 (6)	−0.0489 (6)	0.1104 (7)	4.0 (2)
C23	0.3203 (6)	0.0110 (6)	0.0262 (7)	3.8 (2)
C24	0.2134 (6)	0.0629 (5)	0.0114 (6)	3.0 (2)
C6	−0.1653 (6)	−0.1194 (5)	0.0803 (6)	3.1 (2)
C51	0.3214 (6)	−0.1405 (6)	0.3114 (7)	3.7 (2)
C52	0.3423 (7)	−0.2285 (6)	0.3291 (8)	5.2 (3)
C53	0.4308 (8)	−0.2676 (7)	0.4136 (9)	6.8 (3)
C54	0.4989 (7)	−0.2187 (9)	0.4809 (8)	7.7 (3)
C55	0.4845 (7)	−0.1326 (8)	0.4648 (8)	6.5 (3)
C56	0.3929 (6)	−0.0927 (6)	0.3772 (7)	4.8 (2)
C61	−0.2432 (6)	−0.1561 (5)	0.1290 (7)	3.2 (2)
C62	−0.2602 (7)	−0.1326 (6)	0.2327 (8)	4.7 (2)
C63	−0.3383 (7)	−0.1614 (7)	0.2711 (8)	5.8 (3)
C64	−0.3978 (7)	−0.2150 (6)	0.2065 (8)	5.5 (3)
C65	−0.3838 (7)	−0.2412 (6)	0.1043 (9)	5.4 (3)
C66	−0.3037 (7)	−0.2105 (6)	0.0635 (7)	4.3 (2)
C1D1	0.1258 (5)	0.0988 (5)	0.1707 (6)	3.1 (2)
C2D1	0.0149 (6)	0.1153 (5)	0.1724 (6)	3.1 (2)
C3D1	−0.0180 (6)	0.1717 (6)	0.2629 (8)	4.4 (2)
C4D1	0.0726 (7)	0.1740 (6)	0.3736 (7)	4.2 (2)
C5D1	0.1699 (7)	0.1945 (6)	0.3354 (8)	4.9 (2)
C6D1	0.2073 (7)	0.1359 (6)	0.2500 (7)	4.3 (2)
C7D1	0.1036 (9)	0.0883 (7)	0.4369 (9)	6.8 (3)
C8D1	0.0335 (8)	0.2419 (7)	0.4508 (8)	5.7 (3)
O1D1	−0.0607 (4)	0.0862 (3)	0.1020 (4)	3.3 (1)
O2D1	0.3056 (4)	0.1208 (4)	0.2487 (6)	6.4 (2)
Fe2	0.500	0.500	0.000	4.39 (5)
N3	0.4217 (5)	0.4366 (5)	0.0926 (6)	4.7 (2)
C31	0.3157 (7)	0.4626 (6)	0.1016 (8)	5.2 (3)
C32	0.2933 (7)	0.4033 (6)	0.1754 (8)	5.7 (3)
C33	0.3853 (7)	0.3419 (6)	0.2097 (8)	4.9 (2)
C34	0.4653 (7)	0.3632 (6)	0.1606 (8)	4.4 (2)
C7	0.5697 (6)	0.3118 (6)	0.1676 (8)	4.2 (2)
N4	0.6597 (5)	0.4135 (5)	0.0804 (6)	4.8 (2)
C41	0.7317 (7)	0.3984 (6)	0.0043 (8)	4.9 (2)
C42	0.7626 (7)	0.3080 (6)	−0.0055 (8)	5.0 (3)
C43	0.7136 (7)	0.2672 (6)	0.0601 (8)	5.0 (3)
C44	0.6452 (7)	0.3297 (6)	0.1091 (8)	4.4 (2)
C8	0.7551 (7)	0.4588 (6)	−0.0577 (8)	5.1 (3)
C71	0.6030 (6)	0.2295 (5)	0.2293 (8)	4.2 (2)
C72	0.5394 (8)	0.1664 (5)	0.2022 (9)	5.9 (3)
C73	0.5714 (7)	0.0900 (6)	0.2589 (9)	5.7 (3)
C74	0.6669 (8)	0.0757 (6)	0.3470 (9)	5.9 (3)
C75	0.7315 (8)	0.1350 (7)	0.3746 (8)	5.7 (3)
C76	0.6979 (7)	0.2123 (6)	0.3149 (8)	5.0 (3)
C81	0.8599 (7)	0.4301 (6)	−0.0972 (8)	5.4 (3)
C82	0.9574 (8)	0.4017 (7)	−0.0147 (9)	6.3 (3)
C83	1.0538 (8)	0.3761 (7)	−0.053 (1)	7.8 (4)
C84	1.0528 (9)	0.3801 (7)	−0.163 (1)	8.2 (4)
C85	0.9581 (9)	0.4066 (8)	−0.243 (1)	8.7 (4)
C86	0.8586 (8)	0.4324 (7)	−0.209 (1)	7.0 (3)
C1D2	0.6984 (7)	0.4653 (6)	0.1859 (8)	4.5 (2)
C2D2	0.6294 (7)	0.5389 (6)	0.2080 (8)	4.6 (2)
C3D2	0.6668 (8)	0.5801 (8)	0.3199 (9)	6.9 (3)
C4D2	0.7420 (8)	0.5258 (7)	0.4181 (8)	6.2 (3)
C5D2	0.8402 (9)	0.4790 (7)	0.3731 (9)	6.9 (3)
C6D2	0.8056 (8)	0.4348 (7)	0.2623 (8)	5.7 (3)
C7D2	0.682 (1)	0.4622 (9)	0.454 (1)	10.1 (4)
C8D2	0.787 (1)	0.5799 (8)	0.519 (1)	8.6 (4)
O1D2	0.5398 (5)	0.5707 (4)	0.1381 (6)	6.1 (2)
O2D2	0.8724 (6)	0.3732 (5)	0.2376 (7)	8.2 (2)

[a] Anisotropically refined atoms are given in the form of the isotropic equivalent thermal parameter defined as $(^4/_3)*[a2*B(1,1) + b2*B(2,2) + c2*B(3,3) + ab(\cos \gamma)*B(1,2) + ac(\cos \beta)*B(1,3) + bc(\cos \alpha)*B(2,3)]$.

are significantly longer than the 2.242 (5) Å value found in complex 5a. However, in these mono-N-alkyl derivatives, the
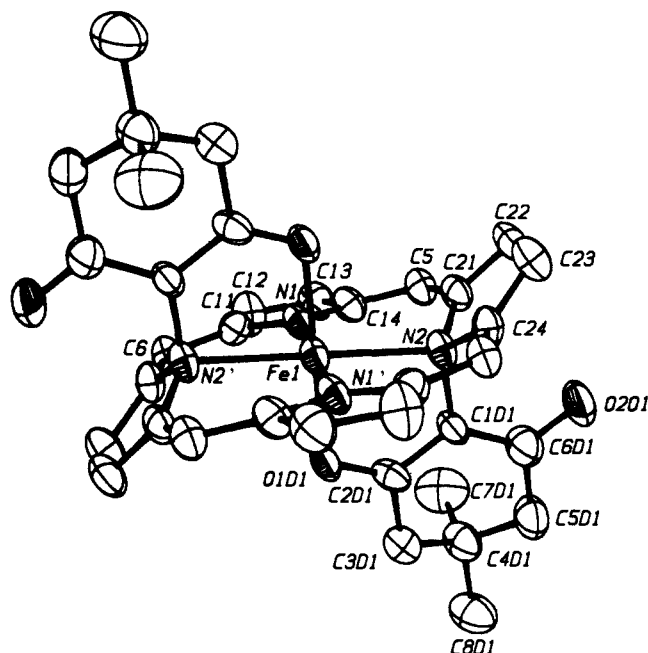

Figure 1. ORTEP plot of one centrosymmetric molecule of complex 5a together with the labeling scheme used. Primed atoms are related to independent atoms by the inversion center. Phenyl rings and hydrogen atoms are omitted for clarity. Ellipsoids are scaled to enclose 30% of the electronic density. The labeling scheme of the second half molecule of complex 5a starts with Fe2, the two pyrrole rings are numbered N3, C31 to C34 and N4, C41 to C44, respectively; C7 and C8 are the methine carbons, and the phenyl carbons are numbered from C71 to C76 and C81 to C86, respectively. The dimedon (X) group starts with C1D2 and goes to O2D2.

metal is always displaced with respect to the plane containing the three nonalkylated porphyrinato nitrogens and also displaced relative to the mean plane containing the alkylated pyrrole nitrogen and the three porphyrinato nitrogens. In contrast, in complex 5a, the iron atom lies in the plane containing the two alkylated and the two nonalkylated nitrogens.

The two Fe–Np bond lengths which are cis to the Fe–N(alkyl) bonds are slightly longer than in all the known six-coordinate low-spin iron(II) porphyrin derivatives (2.000 Å)[16] and even slightly longer than the average bond distance known for the few six-coordinate high-spin iron(II) derivatives (2.063 Å) in which, due to the high-spin state ($S = 2$) of iron, an expanded core is present.[17] Consequently, bis-N-alkylation such as in complex 5a leads to macrocyclic derivatives in which the metal, the two alkylated nitrogens, and the two nonalkylated nitrogens can form a planar entity with an expanded core relative to normal six-coordinate porphyrin derivatives. Such an expanded core is compatible with the formation of six-coordinate high-spin iron(II) complexes.

Although the two individual pyrrole and the two N-alkylated pyrrole rings are almost planar, the mean value of the dihedral angles between their mean planes is 41.3° in the two centrosymmetric molecular units. The mean deviation of the nonalkylated pyrrole ring mean planes relative to the plane containing the four nitrogens and iron (4NFe) is 11.0°, whereas the mean deviation of the N-alkylated pyrrole ring mean planes with respect to the 4NFe plane is as large as 50.3° (the mean value corresponding to the two centrosymmetric entities present in the asymmetric unit). The latter distorsion from planarity is necessary to bring the lone pair of the N-alkylated nitrogens (essentially sp³ hybridized) into an appropriate orientation with iron.

(15) (a) Anderson, O. P.; Lavallee, D. K. *J. Am. Chem. Soc.* **1977**, *99*, 1404–1409. (b) Anderson, O. P.; Lavallee, D. *Inorg. Chem.* **1980**, *16*, 1634–1640. (c) Lavallee, D. K.; Kopelove, A. B.; Anderson, O. P. *J. Am. Chem. Soc.* **1980**, *100*, 3025–3033. (d) Anderson, O. P.; Kopelove, A. B.; Lavallee, D. K. *Inorg. Chem.* **1980**, *19*, 2101–2107.

(16) Scheidt, W. R.; Gouterman, M. *Iron Porphyrins*; Lever, A. B. P., Gray, H. B., Eds.; Addison-Wesley: London, 1983; Vol. 1, p 123.

(17) Scheidt, W. R.; Frisse, M. E. *J. Am. Chem. Soc.* **1975**, *97*, 17–21.

Table III. Selected Bond Lengths (Å), Angles (deg), and Averages with Their Estimated Standard Deviations for Complex 5a[a]

Fe_1-N_1	2.078 (6)	$N_1-Fe_1-N_2$	88.7 (2)
Fe_2-N_3	2.086 (8)	$N_3-Fe_2-N_4$	89.6 (3)
Fe_1-N_2	2.261 (5)	$N_1-Fe_1-O_1D_1$	89.1 (2)
Fe_2-N_4	2.223 (6)	$N_3-Fe_2-O_1D_2$	87.2 (3)
$Fe_1-O_1D_1$	2.002 (5)	$N_2-Fe_1-O_1D_1$	84.1 (2)
$Fe_2-O_1D_2$	1.995 (7)	$N_4-Fe_2-O_1D_2$	84.6 (3)
$N_2-C_1D_1$	1.479 (10)		
$N_4-C_1D_2$	1.523 (11)		

Pyrrole Rings

	Rings N_1 and N_3	Rings N_2 and N_4
$N-C_\alpha$	1.380 (4)	1.444 (4)
$C_\alpha-C_\beta$	1.431 (4)	1.418 (4)
$C_\beta-C_\beta$	1.351 (6)	1.372 (6)
$C_\alpha-C_m$	1.416 (4)	1.382 (4)
$C_\alpha-N-C_\alpha$	106.0 (4)	105.6 (4)
$N-C_\alpha-C_\beta$	109.6 (3)	108.0 (3)
$C_\alpha-C_\beta-C_\beta$	107.3 (3)	109.1 (3)
$N-C_\alpha-C_m$	124.6 (3)	127.0 (3)

Phenyl Rings

C–C	1.387 (3)	C_m-C_{phe}	1.492 (5)	C–C–C	120.0 (1)

Ligands

C_1-C_2/C_1-C_6	1.392 (7)	$C_2-C_3/C_3-C_4/C_4-C_5/C_5-C_6$	1.506 (4)
O_1-C_2/O_2-C_6	1.250 (4)	$Fe-O_1-C_2$	112.6 (4)

[a] Numbering as in Figure 1; C_α and C_β are respectively α and β carbons of pyrrole rings, C_m meso carbons, and C_{phe} quaternary carbon of phenyl groups.

The mean value of the axial Fe–O bond length in the two molecular units is 1.998 (5) Å. This distance is larger than the Fe–O(C–) bond length present in high-spin $Fe(PPIXDME^{13})$-(OCH$_3$) (1.842 (4) Å)[18] but shorter than in the low-spin iron(II) carbonyl adduct $Fe(DPIXDME^{13})(CO)(THF)$ (2.127 (4) Å)[19] and much shorter than in the high-spin iron(II) bis-THF adduct, $Fe(TPP)(THF)_2$, where the Fe–O bond length is 2.351 (3) Å.[18] Despite the large distorsion of the porphyrin ring only the N-(alkyl)–C_2 bond distance is significantly lengthened (mean value 1.444 (4) Å) relative to the $Np-C_\alpha$ bond length (mean value 1.380 (4) Å) whereas the $C_\alpha-C_m$ bond is significantly shortened: C_m-C_α (alkylated pyrrole rings) = 1.382 (4) Å, instead of C_m-C_α (nonalkylated pyrrole rings) = 1.416 (4) Å (Table III). The mean value of the N–C(X group) bond distances of 1.501 (6) Å is similar to those present in other N-alkylated metalloporphyrins.[15]

UV–Vis Spectroscopy of Complexes 5. The UV–vis characteristics of complexes 5 in C_6H_6 at 27 °C are reported in Table I. As expected from iron(II)–N-alkylporphyrins,[20,21] they all exhibit a red-shifted Soret peak (around 465 nm) with a relatively low molecular extinction coefficient. Three peaks around 560, 620, and 750 nm are also observed in the visible region.

Magnetic Susceptibility and EPR of Complex 5a. The magnetic susceptibility of complex 5a was recorded between 4 and 300 K. Above 40 K, the effective magnetic moment is constant and equal to 5.40 ± 0.05 μ_B. Between 40 and 4 K, the moment decreases progressively. It is equal to 4.5 μ_B at 4 K. The compound behaves as expected for a quintet spin state ($S = 2$).[22] The decrease in the lower temperature range is characteristic of a zero field splitting effect which is usually observed for quintet states arising from high spin ferrous ions in distorted octahedral ligand fields.[23]

No EPR transitions are observed in the temperature range

(18) Hoard, J. L.; Hamor, M. J.; Hamor, T. A.; Caughey, W. S. J. Am. Chem. Soc. 1965, 87, 2312–2319.

(19) Scheidt, W. R.; Haller, K. J.; Fons, M.; Mashiko, T.; Reed, C. A. Biochemistry 1981, 20, 3653–3657.

(20) (a) Mansuy, D.; Battioni, J. P.; Dupre, D.; Sartori, E.; Chottard, G. J. Am. Chem. Soc. 1982, 104, 6159–6161.

(21) (a) Balch, A. L.; La Mar, G. N.; Latos-Grazynski, L.; Renner, M. W. Inorg. Chem. 1985, 24, 2432–2436. (b) Lancon, D.; Cocolios, P.; Guilard, R.; Kadish, K. M. J. Am. Chem. Soc. 1984, 106, 4472–4478. Ogoshi, H.; Ketamura, S.; Toi, H. f Aoyama, Y. Chem. Lett. 1982, 495–498.

(22) Eisman, G. A.; Reiss, W. M. Inorg. Chim. Acta 1981, 50, 239–242, and refences cited therein.

(23) Reiss, W. M.; Lang, G. J. Inorg. Chem. 1974, 13, 2150–2153.

Table IV. ^{1}H NMR Characteristics of Complexes 3 and 5[a]

complex	porphyrin ring									phenyl groups					X moiety			
	pyrrole 2H	4H	2H	4H	2H	4H	para 2H	4H	meso 8H	meta 2H	2H	ortho 2H	4H	4H	CH_2 2H	CH_2 2H	CH_2 and CH_3	CH_3 6H
3a[b]	97.6 (800)		82.5 (1100)		76 (1100)		7.2 (50)		11.6 (90)	10.3	9.9	nd[c]			−28.5 (2000)	6.5	to	1
(w$_{1/2}$)[d]																		
3a-d$_{20}$[b]							e	e	11.1 (26)	e	e	e	7.9	4.9 (34)	e	e	e	e
(w$_{1/2}$)[d]																		
3b	89.2 (50)		75.4 (55)		70.5 (55)		3.5 (25)		11.1	10.3	9.8	nd[c]			−28	6.5	to	1
3b-d$_8$[d]	89.5		75.7		70.5													
(w$_{1/2}$)[d]	98		81.8		75		4.9[g] 2.8[f]		11.9 10.9	10.3 9.3	10 8.8	nd[c] nd[c]			−29.5 −26.5	7.5 7.7	to to	1.1 1.5
3c						9.7[g] 3.5[f]												
3d	93.5		81		81													
5a	28.4 (135)		−42.4 (350)		−16.4 (1050)		9.0 (17)		6 (30)			9.5 (160)		4H	35.8 (875)	7.6	+	6.1 (150)[h]
(w$_{1/2}$)[d]	29.3		−42.8		−14.2 −14.5 (55)		0.2[i]		5.9			9.15			35.8	f		6.3
5b	27.5		−41.8		−16.7 −8				5.9			9.5			34.6	7.8		6.2
5c																		

[a] 20 mM in DCCl$_3$ at 20 °C, δ in ppm/Me$_4$Si; dioxane or CH$_3$CN have been used as internal standard to calibrate the proton integration in complexes 3a and 5a. [b] In D$_2$CCl$_2$. [c] nd = not detected. [d] Half-width in Hz. [e] Not measurable because of an overlapping of the signals with another one. [f] ^{1}H NMR in CH$_2$Cl$_2$, signal at 3.5 ppm has been used as reference. [g] CH_3-para (6H). [h] Determined from complex 5a-d$_{20}$. [i] CH_3-para (12H). [j] ^{1}H NMR in HCCl$_3$, 10% DCCl$_3$ has been added as internal reference.
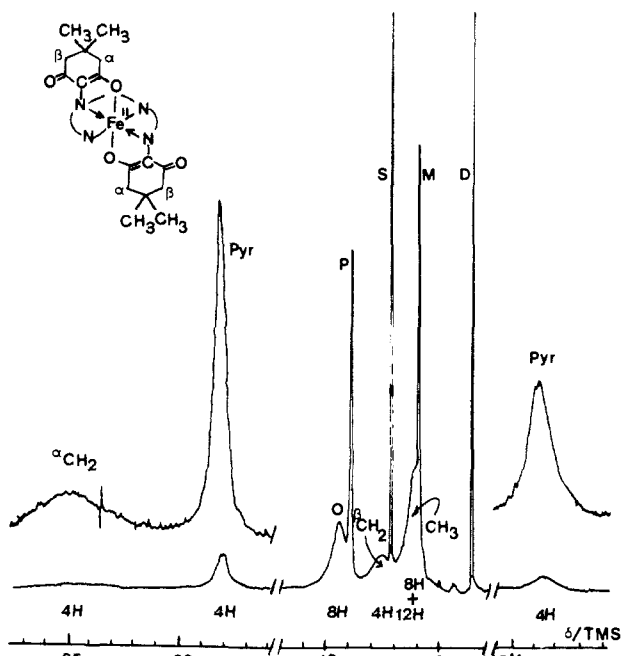
Figure 2. ^{1}H NMR spectrum of complex **5a** (in DCCl$_3$, 20 °C, δ in ppm from Me$_4$Si). For the protons of the porphyrin ring: O = ortho, M = meta, P = para, Pyr = pyrrole. A known amount of dioxane (D) has been used as internal standard for proton integration. S = HCCl$_3$.

4.2–300 K. This fact confirms the quintet state as a ground state, with a zero field splitting larger than the X-band microwave frequency.

^{1}H NMR Spectra of Complexes 5. The ^{1}H NMR spectra of complexes **5** are also characteristic of their paramagnetic nature with the large range (36 to −43 ppm) and broad shapes of the signals. The assignments of these signals have been made by comparison of the spectra of complexes **5** with those of their analogues **5a-d_{20}** and **5b-d_8** prepared from the tetraarylporphyrin

selectively deuterated on the aryl groups (d_{20}) or on the pyrrole rings (d_8). The ^{1}H NMR data are reported in Table IV.

In agreement with the centrosymmetric structure, the pyrrole protons of all complexes **5** appeared as two broad signals (4 H each), one of them appearing downfield around 28 ppm from Me$_4$Si and the other one upfield around −42 ppm. This assignment was confirmed by the absence of these two signals in the ^{1}H NMR spectrum of complex **5b-d_8**. The para H of phenyl rings of complex **5a** which appeared as a sharp signal ($W_{1/2}$ = 17 Hz) at 9.0 ppm (4 H) was unambiguously identified since this signal was missing in the spectra of complexes **5b** and **5c** (Figure 2). Two others signals (8 H each) around 9 and 6 ppm are present in the spectra of all complexes **5** and are lacking in those of complex **5a-d_{20}**. They were respectively assigned to the ortho and meta H of phenyl rings, on the basis of their half-widths. Effectively, the ortho-aryl protons which are closest to the paramagnetic iron center are more efficiently relaxed and then appear as a broad signal ($W_{1/2}$ = 160 Hz) while the meta-aryl proton signal is sharper ($W_{1/2}$ = 30 Hz).

The signals of protons of the X moiety were identified by comparison between the spectra of complexes **5a-d_{20}** and **5b-d_8**. Only three signals at about 35 (4 H), 7.5 (4 H), and 6.1 ppm (12 H) were present in both spectra and in all complexes **5**. On the basis of their integration, the latter signal was assigned to the dimethyl groups and the two others to the methylene groups of the two X moieties. The methylene groups which are closer to the paramagnetic center give a very broad signal ($W_{1/2}$ = 875 Hz) at low field (around 35 ppm). The other methylene groups lead to a sharper signal at 7.6 ppm which is in part masked by the meta aryl protons signal.

Electrochemical Oxidation of Complexes 5. The cyclic voltammogram of **5a** exhibits a single wave which can be described as a one-electron reversible step with $E_{1/2}$ = 0.41 V vs. SCE (Figure 3A). Coulometry at a platinum gauze (controlled potential set to 0.6 V vs. SCE) gives 0.99 as number of electrons exchanged per molecule. Spectroelectrochemistry confirms the reversible transformation of complex **5a** into a new red complex **6a**. Indeed, upon oxidation of complex **5a** at + 0.6 V, the visible spectrum of complex **6a** exhibiting bands at 440 and 540 nm[24]
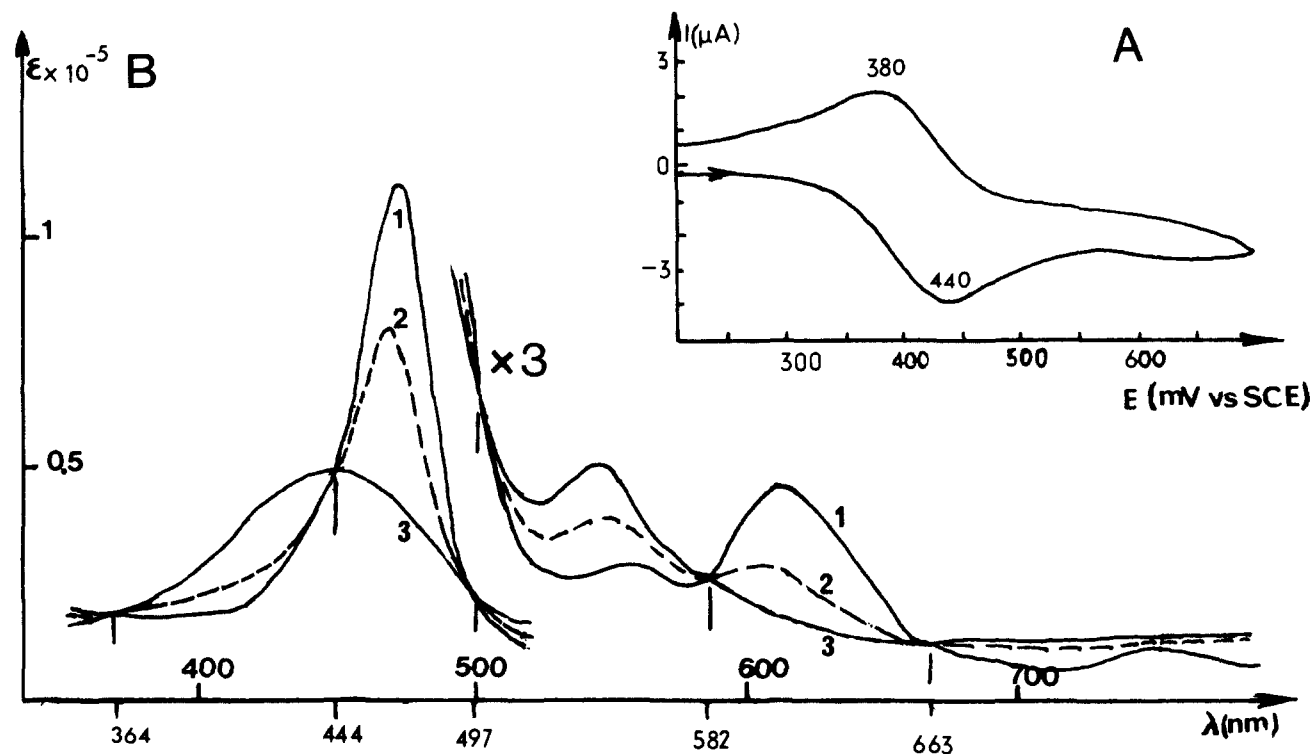

Figure 3. (A) Cyclic voltammogram of complex **5a** (1 mM in CH$_3$CN, 0.2 M LiClO$_4$) at a glassy carbon electrode. Potential sweep rate 0.2 V/s. (B) spectroelectrochemical oxidation of complex **5a** (0.4 mM in CH$_3$CN, 0.2 M LiClO$_4$) at a platinum minigrid electrode. Potential: 0.6 V. Spectra 1–3 were obtained after respectively 0, 5, and 10 min.
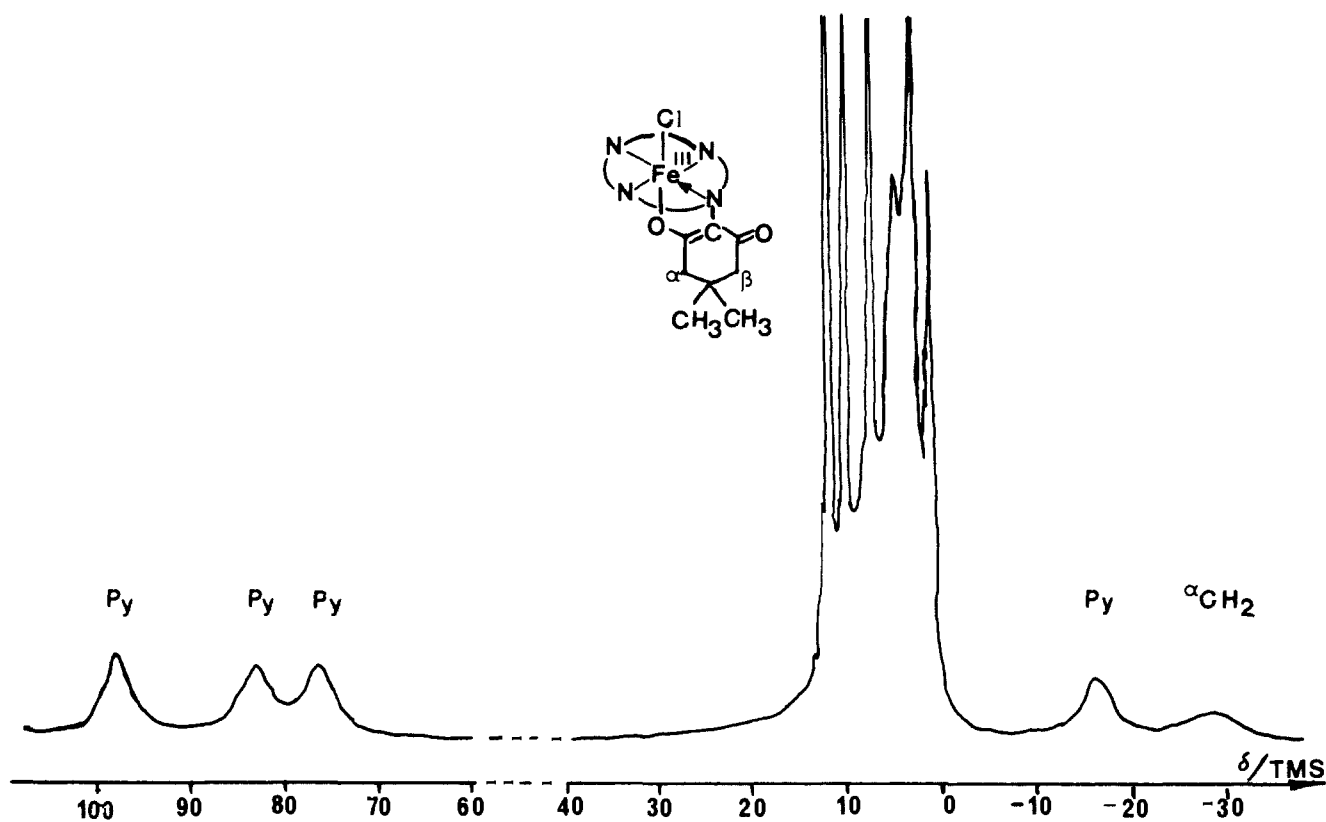
Figure 4. ^{1}H NMR spectrum of complex **3a** (in DCCl$_3$, 20 °C); Py = pyrrole.

is obtained with five clean isosbestic points at 364, 444, 497, 582, and 663 nm (Figure 3B). Spectrum of complex **5a** is regenerated upon reduction of complex **6a** at 0 V with the same set of isosbestic points.

Although we did not try to isolate and completely characterize complex **6a**, its electrochemical characteristics are compatible with a bismetallocyclic structure like complex **5a** but with a Fe^{III} state of the iron (Scheme I). Similar results were obtained from complexes **5b** and **5c** which led to complexes **6b** and **6c**, respectively[24] (Table I).

II. Reaction of C$_6$H$_5$I=X (1) with Iron(III)-Porphyrins: Preparation of Monometallocyclic Iron–Porphyrin Complexes, 3. Although reaction of the iodonium ylide **1** with various Fe^{II} porphyrins has led almost exclusively to the bismetallocyclic Fe^{II} complexes **5** (for porphyrin TPP, TpClPP and TTP), we found that the reaction of Fe^{II}(TMP) with **1** failed to give a similar complex. Even the use of a very large excess of **1** (80 equiv) did not provide a bismetallocyclic Fe^{II} complex analogous to **5a**, presumably because of the greater hindrance of the TMP derivatives. In fact, this reaction led to a monometallocyclic *N*-alkylporphyrin-Fe^{III} complex **3d** (after aerobic HCl treatment of the crude reaction mixture) (see below structure evidence).

We then found that such monometallocyclic complexes **3** could be easily obtained in a more general manner upon reaction of **1** with Fe^{III}(porphyrin)(ClO$_4$) complexes generated in situ from Fe(porphyrin)(Cl) and AgClO$_4$ in deaerated CH$_2$Cl$_2$. For instance, reaction of Fe(TPP)(ClO$_4$) with 20 equiv of **1** led, after HCl treatment, to a 60% yield of **3a** together with minor amounts of **5a** (5%). By using a smaller excess of **1** (10 equiv), complex **3a** was obtained almost quantitatively within 2 h at 20 °C. A similar procedure applied to Fe^{III}(TpClPP)(ClO$_4$) and Fe^{III}(TTP)(ClO$_4$) led respectively to complexes **3b** and **3c** (70% yield). Complex **3d** was prepared from reaction of **1** with Fe(TMP)(ClO$_4$), but in that case an excess of 50 equiv was required to obtain a satisfactory yield (60%).

Structure and Spectral Properties of Complexes 3. The green-brown complexes **3a**, **3b**, and **3c** exhibit UV–vis spectra (Table I) with a red-shifted Soret peak around 456 nm with a relatively small molar extinction coefficient and 4 peaks in the visible region around 525, 580, 655, and 730 nm. The spectrum of complex **3d** is similar, but all its peaks are slightly blue-shifted. These spectra are slightly different from those of the classical *N*-methyl- or *N*-phenylporphyrin–iron(III) complexes,[21] but they are similar to that of the only *N*-alkylporphyrin–iron(III) complex for which such a metallocyclic structure has been very recently proposed.[25]

Complexes **3** are high-spin Fe^{III} complexes ($S = \frac{5}{2}$) as shown for **3a** and **3d** by the value of their magnetic moment ($\mu_{eff} = 5.9$ μ_B in HCCl$_3$ solution at 20 °C) measured by the Evans method.[26] Their EPR spectra recorded on the complexes in the powder state at 4.2 K respectively exhibit signals at $g = 4.168$ and 4.056, each corresponding to the isotropic signal of a high-spin iron(III) complex with rhombic symmetry.

Structures of complexes **3** have been deduced from (i) their elemental analysis, (ii) their mass and ^{1}H NMR spectra and (iii) the complete transformation of complexes **3a**, **3b**, and **3c** into complexes **5a**, **5b**, and **5c**, respectively, upon reaction of the one-electron reduction products of complexes **3** with **1**. Because of the steric hindrance caused by its ortho methyl groups, complex **3d** fails to react with compound **1**. However, its structure is assumed to be identical with those of other complexes **3** on the basis of its elemental analysis, its mass spectrum, and the great similarity of its UV–vis and ^{1}H NMR spectra with those of complexes **3a–3c**.

The elemental analysis (C, H, N, Cl) of all complexes **3** corresponds to the formula Fe(porphyrin)(C$_8$H$_{10}$O$_2$)(Cl),H$_2$O, indicating the formal incorporation of only one X moiety into Fe-(porphyrin)Cl and a residual solvation by one water molecule (see Experimental Section).

(24) UV–vis (C$_6$H$_6$, 27 °C, λ(nm), ε (mM^{-1}·cm^{-1})) **6a**: 440 (50.2), 540 (17), 580 (sh); **6b**: 440 (68.3), 540 (19.5), 575 (sh); **6c**: 450 (71.5), 543 (22.4), 583 (sh).

(25) Mashiko, T.; Dolphin, D.; Nakano, T.; Traylor, T. G. *J. Am. Chem. Soc.* **1985**, *107*, 3735–3736.

(26) (a) Evans, D. F. *J. Chem. Soc.* **1959**, 2003–2005. (b) Brevard, C.; Granger, P. *Handbook of High Resolution Multinuclear NMR*; John Wiley: New York, 1981; p 41.

The mass spectra (impact direct inlet) of complexes **3a**, **3b**, and **3c** do not exhibit the molecular peak but only peaks corresponding to the loss of the axial chlorine ligand (i.e., M^+-Cl) and to the loss of the X group (i.e., M^+-Cl-X) (Table I); whereas the mass spectrum of complex **3d** (desorption chemical ionization technique, I^-, CH_4) exhibits a molecular cluster peak at m/e 1011 and 1009 (3%) with an isotopic ratio characteristic of the presence of a chlorine atom and fragments at m/e 975 ($M^+ + 1 - Cl$) (100%) and 836 ($M^+ - Cl - X = Fe(TMP)$) (18%). All the mass spectra of complexes **3** exhibit a fragment corresponding to Fe(porphyrin) indicating that the porphyrin ring remains intact in complexes **3** and disfavors any structure which would have derived from an addition of the X carbene moiety on a pyrrole double bond or from its insertion into a C–H pyrrolic or C–aryl simple bond.

The reduction of complexes **3a**, **3b**, **3c**, and **3d** by sodium dithionite in a biphasic medium (H_2O, CH_2Cl_2) gives new complexes, respectively **4a**, **4b**, **4c**, and **4d** which are stable under these reductive conditions but are rapidly reoxidized to the starting complex in the presence of O_2 and Cl^-. The reversible transformation **3** ⇌ **4** is confirmed by cyclic voltammetry in DMF solution ($E_{1/2}$ between –0.3 and –0.1 V vs. SCE)[27] (Table I). The addition of a methylene chloride solution of **4a**, **4b**, or **4c** to an excess of compound **1** gives *immediately and quantitatively* the corresponding bismetallocyclic iron(II) complex **5a**, **5b**, or **5c** whereas **4d** fails to react with compound **1** (Scheme I).

Taken altogether, these data support the monometallocyclic structure of complexes **3**, indicated in Scheme I, where a O–C–C moiety derived from the X group is inserted into a Fe–N bond of the starting ferric porphyrin. The ^1H NMR spectra of complexes **3** are in complete agreement with this structure.

^1H NMR Spectra of Complexes 3. As for complexes **5**, the ^1H NMR spectra of complexes **3** are also characteristic of paramagnetic compounds with broad signals appearing over a 130 ppm range. For a complete assignment of the signals it has been necessary to compare the spectra of complexes **3** with those of their analogues **3a-d_{20}** (**3a** deuterated on the phenyl groups) and **3b-d_8** (**3b** deuterated on the pyrrole rings) and to study the ^2H NMR spectra of the two latter complexes. The ^1H NMR characteristics of complexes **3** are listed in Table IV, and the ^1H NMR spectrum of complex **3a** is shown in Figures 4 and 5.

In agreement with the C_s symmetry of complexes **3**, their pyrrole protons appear as four signals (2 H each), three of them at very low field, between 98 and 76 ppm downfield from Me_4Si, the fourth one at high field, between –8 and –16 ppm (Figure 4). This assignment, made on the basis of the absence of these signals in the ^1H NMR spectra of complex **3b-d_8**, was confirmed by a study of the ^2H NMR of complex **3b-d_8** which exhibits only four signals of equal intensity at the same chemical shifts. The para H of the phenyl groups of complex **3a** appear as two signals at 7.2 (2 H) and 3.5 (2 H). These two signals are absent in the spectra of complexes **3b** and **3d**. They are respectively replaced by two signals at 3.5 (2 × 3 H) and 2.8 (2 × 3 H) ppm in complex **3d** which are assigned to the para methyl protons. The signals of the meta H protons of the phenyl groups appear as a set of three signals (4 H, 2 H, and 2 H) between 11.6 and 8.8 ppm. They are present in the spectra of all complexes **3** and missing in complex **3a-d_{20}**.

Because of the large line width of the signals and the presence of other broad signals in the same region, the resonances of ortho H protons could not be directly determined on the ^1H NMR spectra of **3a**, **3b**, or **3c**. However their presence between 1 and 12 ppm was shown by integration of the signals in this region. Similarly, the presence of the signals of the ortho CH_3 groups of complex **3d** in the 1–12 ppm region could only be detected by integration of the signals in this region. Finally, the ortho H protons of the aryl groups have been localized only on the ^2H NMR spectrum of complex **3a-d_{20}** where they appear as two very broad signals around 7.9 and 4.9 ppm. Since the signal at 7.9 ppm overlaps with those of para ^2H, only the half-width of the
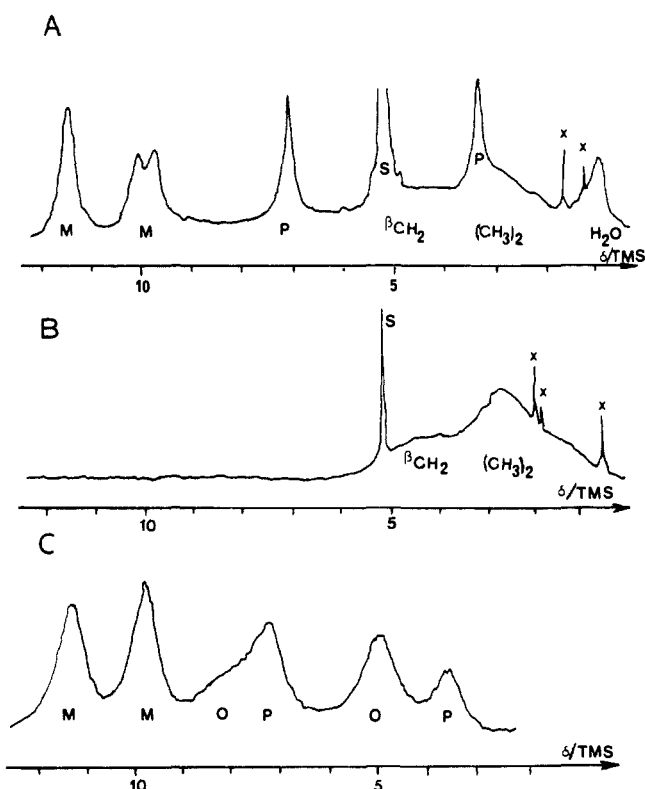
Figure 5. (A) ^1H NMR spectrum of complex **3a** (in $DCCl_3$, 20 °C) (0–12 ppm region). (B) ^1H NMR spectrum of complex **3a-d_{20}** (in $DCCl_3$, 20 °C). (C) ^2H NMR spectrum of complex **3a-d_{20}** (in D_2CCl_2, 20 °C). O = ortho, M = meta, P = para, S = solvent, x = impurity, H_2O (disappears upon addition of D_2O).

signal at 4.9 ppm could be measured ($W_{1/2} = 34$ Hz) (Figure 5C). This would lead to an extrapolated half-width of the corresponding resonances in ^1H NMR around 1400 Hz which would explain why these resonances of the ortho H phenyl protons could not be directly detected in the ^1H NMR spectra of complex **3a** (Figure 5A).
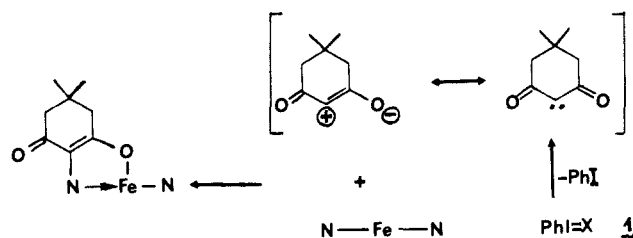
As far as the signals of group X are concerned, a very broad resonance ($W_{1/2} = 2000$ Hz) was observed around –28 ppm (Figure 4) in the spectra of all complexes **3**. This signal (2 H) is assigned to the methylene group of the X moiety which is closest to the paramagnetic center. The protons of the other methylene group and of the two methyl groups appear in the spectrum of complex **3a-d_{20}** as two very broad signals (Figure 5B) between 6.5 and 1 ppm and centered at 4.5 and 2.9 ppm. In the spectra of nondeuterated complexes **3**, they are superimposed to those of the ortho H phenyl groups (Figure 5A). The ^1H NMR spectra of complexes **3** are similar to those reported for [Fe^{III}(N-alkyl-TPP)(Cl)]$^+$ cationic complexes.[21a] They do not allow one to exclude a [Fe^{III}(N-XH-TPP)(Cl)]$^+$ structure for complexes **3** derived from the formula indicated in Scheme I by dissociation of the Fe–O bond and protonation of the oxygen atom. However, conductimetry measurements performed on complex **3a** (conductivity of **3a** 10^{-3} M in DMF almost equal to that of pure DMF) are completely inconsistent with such a cationic structure. Moreover, the great stability of complexes **3** at room temperature and their EPR signals (g around 4.1) indicative of a rhombic symmetry are in agreement with the bridged structure Fe(N-X-TPP)(Cl) but not with a cationic structure [Fe(N-XH-TPP)(Cl)]$^+$, since previously described [Fe(N-alkyl-TPP)(Cl)]$^+$ complexes, were found stable only below –40 °C and exhibit $g = 5.6$ and 2.1 EPR signals indicative of an axial symmetry.[21] All these data clearly indicate the bridged structure of Scheme I for complexes **3**.

Discussion

The aforementioned results show that the reaction of the io-

(27) UV–vis (DMF, 27 °C, λ (m), ε (mM^{-1}·cm^{-1})) **4a**: 461 (141), 640 (14.7); **4b**: 467 (169), 650 (18); **4c**: 463 (141), 637 (13.8); **4d**: 449 (128), 558 (7.9), 622 (6.2), 673 (3.6).

Reaction of C Equivalent of Iodosylbenzene with Ir–Porphyrins

J. Am. Chem. Soc., Vol. 108, No. 18, 1986 5605

Scheme II

Chart I

$Fe^{II}(N-R TPP)Cl$

Scheme III

donium ylide $C_6H_5I=X$, a carbon equivalent of $C_6H_5I=O$, with iron(II)– or iron(III)–porphyrins provides an easy access to porphyrin complexes exhibiting a new type of metallocyclic Fe–O–C–C–N structure. Both monometallocyclic and bis-metallocyclic complexes could thus be prepared, the iron being either in the ferric or ferrous state.

Although its mechanism is not yet known, the formation of the five-membered F–O–C–C–N metallocycle can be very formally written as an insertion of a $^-O-C=C^+$ moiety of the carbene X derived from $C_6H_5I=X$ into a Fe–N bond of the starting iron–porphyrin (Scheme II).

The ferric monometallocyclic complexes **3** have been isolated and completely characterized. The reversible passage to the corresponding ferrous complexes has been shown by cyclic voltammetry and spectroelectrochemistry. The latter complexes, **4**, have been so far only characterized by UV–vis spectroscopy mainly because of their instability toward dioxygen compared to complexes **3**. A more complete study of their structures, spectral characteristics, and reactivity is underway. However, one of their properties particularly relevant to Scheme I which is demonstrated by this study is the fast and complete reaction with $C_6H_5I=X$, leading to the bismetallocyclic complexes **5**. On the contrary, complex **3** fails to react with $C_6H_5I=X$ under identical conditions. The ferrous bismetallocyclic complexes **5** have been also completely characterized. They are very stable in aerated solutions, unlike to the ferrous monometallocyclic complexes **4**. The ferric bis-metallocyclic complexes **6** have been only characterized so far by UV–vis spectroscopy. The reversible passage **5** $\rightleftharpoons$ **6** has been shown by cyclic voltammetry and spectroelectrochemistry. The fact that the more stable state for the monometallocyclic complexes is the ferric state, whereas the more stable state for the bis-metallocyclic complexes is the ferrous state, is in agreement with the redox potentials of the **3** $\rightleftharpoons$ **4** (–100 to –300 mV) and **6** $\rightleftharpoons$ **5** (+300 to +600 mV) reactions.

The high reactivity of complexes **4** toward either dioxygen or $C_6H_5I=X$ when compared to complexes **3** and the very difficult oxidation of complexes **5** (see redox potentials, Table I) into complexes **6** explain why complexes **3** and **5** were the only final complexes isolated from reactions between iron–porphyrins and $C_6H_5I=X$. In reactions between Fe^{III}(porphyrin)(ClO$_4$) and $C_6H_5I=X$, the ferric complexes **3** are formed almost quantitatively. In reactions performed between Fe^{II}–porphyrins and $C_6H_5I=X$ under anaerobic conditions, it is likely that complex **4** is formed in steady-state concentrations and reacts very rapidly with $C_6H_5I=X$ leading to complex **5** which is almost the only product isolated under these conditions. In the particular case of Fe^{II}(TMP), the proposed intermediate complex **4d** would fail to react with $C_6H_5I=X$ because of the steric hindrance caused by the ortho-methyl groups of the meso phenyl substituents. Instead, this intermediate should be rapidly oxidized to complex **3d**, explaining why it was the only product isolated from the reaction.

It is noteworthy that complexes **3** and **4** have a different redox behavior when compared to iron–N-alkylporphyrin complexes in general. The latter complexes have been reported to be stable in the ferrous state[15d] and very unstable in the ferric state[21] in agreement with their higher redox potentials (from +500 to –60 mV).[15d,21b,28] The much greater reactivity of complexes **4** toward
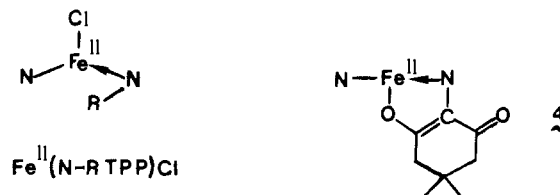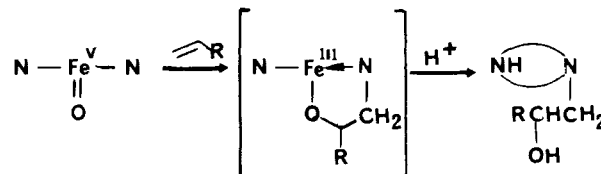
dioxygen when compared to Cl–Fe^{II}–N-alkyl-TPP complexes[15d] could be due at least in part to the much more difficult access of iron in the latter where the two axial positions are hindered by the chloride ligand on one side and by the N–R group on the other side. On the contrary, in complexes **4**, one axial position is readily accessible (Chart I) explaining its great reactivity not only toward dioxygen but also toward $C_6H_5I=X$.

The aforementioned results completely establish the existence of metallocyclic iron–porphyrin complexes exhibiting a Fe–O–C–C–N structure and give structural data for one of them. They also give spectroscopic data and reactivity characteristics which should be important for the isolation and study of analogous metallocyclic complexes which have been postulated as intermediates in the formation of green porphyrin pigments in the liver of animals treated by alkenes[29] (Scheme III). The formation of such green N-substituted porphyrins has been recently described upon model reaction of alk-1-enes with iodosoarenes in the presence of iron–tetraarylporphyrins.[25,30] The iron complexes which are formed in these model reactions and which lead to the isolated N-substituted porphyrins by acid demetalation have been characterized so far by UV–vis and EPR spectroscopy.[25] Their UV–vis characteristics are similar to those of the metallocyclic ferric complexes described in this paper. Moreover, contrary to ferric–N-alkylporphyrin complexes described previously,[21] they are stable at room temperature.[25] Our results showing the exceptional stability of the Fe^{III}–O–C–C–N metallocyclic complexes allow one to understand this property.

Experimental Section

Materials. Compound **1**, PhI$=X$ (X = $C_8H_{10}O_2$), was prepared according to ref 14. TPPH$_2$, TTPH$_2$, and TpClPPH$_2$ were synthesized according to Alder's method[31] and TMPH$_2$ according to Badger's.[32] TPP-d_{20} and TpClPP-d_8 were synthesized according to ref 33. They were made chlorine free by Smith's procedure,[34] and they were metalated by FeCl$_2$·4H$_2$O in DMF.[35]

Physical Measurements. UV–vis spectra were obtained in toluene or in CH$_2$Cl$_2$ by using a Kontron Uvikon 810 or an Aminco DW 2 spectrophotometer.

Mass spectra were recorded on a VG 70-250 double-focussing in-

(28) Kuila, D.; Kopelove, A. B.; Lavallee, D. K. *Inorg. Chem.* **1985**, *24*, 1443–1446.

(29) (a) Ortiz de Montellano, P. R.; Kunze, K. L.; Beilan, H. S.; Wheeler, C. *Biochemistry* **1982**, *23*, 1331–1339. (b) Ortiz de Montellano, P. R.; Correia, M. A. *Annu. Rev. Pharmacol. Toxicol.* **1983**, *23*, 481–503.

(30) Mansuy, D.; Devocelle, L.; Artaud, I.; Battioni, J. P. *Nouv. J. Chem.* **1985**, *9*, 711–716.

(31) Alder, D. A.; Longo, F. R.; Finarelli, J. D.; Goldacher, J.; Assour, J.; Korsakoff, L. *J. Org. Chem.* **1967**, *32*, 476.

(32) Badger, G. M.; Jones, R. A.; Laslett, R. L. *Aust. J. Chem.* **1964**, *17*, 1028–1035.

(33) Fajer, J.; Borg, D. C.; Forman, A.; Felton, R. H.; Vegh, L.; Dolphin, D. *Ann. N. Y. Acad. Sci.* **1973**, *206*, 349–364.

(34) (a) Barnett, G. H.; Hudson, M. F.; Smith, K. M. *Tetrahedron Lett.* **1973**, 2887–2888. (b) Abraham, J. R.; Hawkes, G. E.; Hudson, M. F. *J. Chem. Soc., Perkin Trans. 1* **1975**, 1401–1403.

(35) Fleischer, E. B.; Palmer, J. M.; Srivastava, T. S.; Chatterjee, A. *J. Am. Chem. Soc.* **1971**, *93*, 3163–3167.

5606 *J. Am. Chem. Soc., Vol. 108, No. 18, 1986*

Battioni et al.

strument (from VG Analytica, Manchester, UK) equipped with a fast-atom bombardment gun (from Ion Tech Ldt, Teddindton, UK). The scanning acquisition parameters were the following: accelerating voltage, 4 KV; scan time, 15 s/decade; interscan time, 2 s. The FAB gun was operated with xenon (N45, Air Liquide, France) at 7.5 KV and 1.2 mA. The apparatus was calibrated with cesium iodide, and different matrices were used: glycerol and thioglycerol or dimethyl sulfoxide. All chemical reagents used were of the best available quality.

Elemental analyses were done by the Service de Microanalyse du C.N.R.S. at Gif sur Yvette.

^{1}H NMR spectra for complexes 10^{-2} M in $CDCl_3$ or CD_2Cl_2 were run at 20 °C on a Bruker WH 250 spectrometer operating at 250 MHz; chemical shifts are reported in ppm downfield of Me_4Si (sweep width 5000 Hz, 256–1024 scans, 60 pulses, 3.0 Hz/pt resolution, 32K point memory blocks, acquisition time 0.32 s, repetition delay 1 s). ^{2}H NMR spectra were run at 38.4 MHz (sweep width 5680 Hz, 20 000–30 000 scans, 60 pulses, 0.71 Hz/pt resolution, 16K point memory blocks, acquisition time 1.4 s with broad band of ^{1}H decoupling, repetition delay 1 s). $DCCl_3$ or D_2CCl_2 (10%) was used as internal reference.

Magnetic susceptibility measurements were carried out with a Faraday type magnetometer equipped with a continuous flow cryostat in the temperature range 4.2–300 K. The polycrystalline powder samples weighed about 3 mg. The applied magnetic field was in the range 0.1–0.7 T. The independence of the susceptibility against the magnetic field was checked at room temperature. Mercuritetrakis(thiocyanato)cobaltate-(III) was used as a standard susceptibility. The magnetic data were corrected for the molecular diamagnetism estimated as -860×10^{-6} $cm^3 \cdot mol^{-1}$.

The EPR properties were checked with a Bruker ER 200 D spectrometer equipped with a continuous flow cryostat and working in X-band, in the temperature range 4.2–300 K.

Cyclic Voltammetry and Coulometry. Experiments were carried out with a Princeton Applied Research Model 173 potentiostat, monitored with an Apple //e microcomputer and a P.A.R. Model 276 GPIB interface. A three electrode system was used with a platinum disk or a glassy carbon disk working electrode, a platinum wire counter electrode, and a saturated calomel electrode (filled with NaCl instead of KCl to prevent crystallization of $KClO_4$). The reference electrode was separated from the bulk of the solution by a fritted glass bridge and filled with the solvent and supporting electrolyte at appropriate concentration. For coulometry experiments the counter electrode was separated by a bridge with a Nafion membrane, filled with the same supporting electrolyte solution. The spectroelectrochemical device (analogue to Lexa's[36] consisted in a three electrodes cell, with as compartment of electrolysis a quartz cell (optical length, 0.5 mm; inner volume, 0.08 mL). The working electrode was a platinum minigrid. Except for the oxidation of **5a**, all solutions were deaerated by an argon stream before experiments, then protected by a blanket of argon. Dimethylformamide was distilled under reduced pressure; acetonitrile (quality: HPLC grade S), purchased from Rathburn Chem. Limited, and reagent grade quality $LiClO_4$ and LiCl, purchased from Fluka Co., were used without further purification.

X-ray Analysis. Suitable single crystals of **5a** were obtained by slow evaporation of solvents from CH_2Cl_2–pentane solutions at room temperature.

A systematic search in reciprocal space using a Philips PW 1100/16 automatic diffractometer showed that crystals of **5a** belong to the triclinic system. The unit-cell dimensions and their standard deviations were obtained and refined at room temperature with Cu K_α radiation ($\lambda = 1.5405$ Å) by using 25 carefully selected reflections and the standard Philips software. Final results for $C_{60}H_{48}N_4O_4Fe$ were the following: mol wt 944.9, $a = 12.785$ (3) Å, $b = 15.963$ (4) Å, $c = 12.104$ (3) Å, $\alpha = 91.77$ (2)°, $\beta = 105.46$ (2)°, $\gamma = 78.71$ (2)°, $V = 2334$ Å^3, $Z = 2$, $d_{calcd} = 1.344$ g·cm^{-3}, $d_{obsd} = 1.32 \pm 0.02$ g·cm^{-3}, $\mu = 30.11$ cm^{-1}, $F_{000} = 988$, space group P$\bar{1}$.

A parallelepipedic crystal of $0.32 \times 0.18 \times 0.04$ mm was sealed in a Lindemann glass capillary and mounted on a rotation free goniometer head. All quantitative data were obtained from a Philips PW 1100/16 four circle automatic diffractometer, controlled by a P 852 computer, by using a graphite monochromator and standard software. The vertical and horizontal apertures in front of the scintillation counter were adjusted so as to minimize the background counts without loss of net peak intensity at the 2σ level. The total scan width in the $\theta/2\theta$ flying step-scan used was $\Delta\theta = 0.9 + 0.143$ tg (θ) deg with a step width of 0.04 deg and a scan speed of 0.015 deg·s^{-1}. A total of 6529 hkl, $\bar{h}kl$, $h\bar{k}l$, and $\bar{h}k\bar{l}$ reflections were recorded ($5° < \theta < 57°$). The resulting data set was transfered to a PDP 11/60 computer, and for all subsequent computations with the

exception of a local data-reduction program, the Enraf-Nonius SDP/V18 package was used.[37]

Three standard reflections measured every hour during the entire data-collection period showed no significant trend. The raw step-scan data were converted to intensities by using the Lehmann–Larsen method[38] and then corrected for Lorentz polarization and absorption factors, the latter computer by the numerical integration method of Busing and Levy[39] (transmission factors between 0.43 and 0.88). A unique data set of 3255 reflections having $(I) > 3\sigma(I)$ was used for determining and refining the structure.

The structure was solved by using the heavy atom method. After refinement of the heavy atoms, a difference-Fourier map revealed maxima of residual electronic density close to the positions expected for hydrogen atoms; they were introduced in structure factor calculations by their computed coordinates (C–H = 0.95 Å) and isotropic temperature factors of $B_{eqv}(C) + 1$ Å^2 but not refined. Full least-squares refinement converged to $R(F) = 0.076$ and $Rw(F) = 0.095$ ($\sigma(F^2) = (\delta_{count}^2 + (pI)^2)$. The unit weight observation was 1.82 for $p = 0.07$. A final difference map revealed no significant maxima. The scattering factors coefficients and anomalous dispersion coefficients come respectively from ref 40 and 41.

General Procedure for Preparation of Complexes 3: Fe(P)(C$_8$H$_{10}$-O$_2$)(Cl). To a deaerated solution of 0.2 mmol of Fe^{III}(porphyrin)(Cl) in 80 mL of CH_2Cl_2 was added 0.3 mmol of anhydrous $AgClO_4$. The solution was stirred under argon for 0.5 h at room temperature and then added to 2 mmol of compound **1** and 0.3 mmol of $AgClO_4$ previously deaerated by a bubbling of argon. After stirring for 2 h at 20 °C, the solution was filtered and stirred during 0.25 h in the presence of 5 mL of concentrated HCl dissolved in 20 mL of CH_3OH. The organic layer was washed with water and dried over Na_2SO_4. After filtration and evaporation of solvents, the crude product was purified by a SiO_2 column chromatography (CH_2Cl_2/ethyl acetate, 95:5 as eluent) and precipitated by addition of pentane to a CH_2Cl_2 solution.

Complexes **3a**, **3b**, and **3c** were obtained as brown powders in 70–90% yield. Complex **3d** which did not crystallize even in pure pentane was dissolved in C_6H_6 and lyophilized under high vacuum (60% yield). Complex **3a** Fe(TPP)(C$_8$H$_{10}$O$_2$)(Cl)·H$_2$O: Anal. Calcd (found) for $C_{52}H_{40}N_4FeClO_3$: C, 72.60 (72.39); H, 4.65 (4.42); N, 6.51 (6.86); Cl, 4.13 (4.50). Complex **3b** Fe(TpClPP)(C$_8$H$_{10}$O$_2$)(Cl)·H$_2$O: Anal. Calcd (found) for $C_{52}H_{34}N_4FeCl_5O_3$: C, 62.55 (62.47); H, 3.61 (3.59); N, 5.72 (6.01); Cl, 17.80 (18.00). Complex **3c** Fe(TTP)(C$_8$H$_{10}$O$_2$)(Cl)·H$_2$O: Anal. Calcd (found) for $C_{56}H_{48}N_4FeClO_3$: C, 73.40 (72.95); H, 5.28 (5.17); N, 6.11 (6.44); Cl, 3.87 (3.92). Complex **3d** Fe-(TMP)(C$_8$H$_{10}$O$_2$)(Cl)·H$_2$O: Anal. Calcd (found) for $C_{64}H_{64}N_4FeClO_3$: C, 74.74 (74.80); H, 6.23 (6.44); N, 5.45 (5.05); Cl, 3.45 (2.94).

General Procedure for Preparation of Complexes 5: Fe(P)(C$_8$H$_{10}$O$_2$)$_2$ **(1) from Fe^{III}(porphyrin)(Cl).** To a deaerated solution of 0.6 mmol of Fe^{III}(porphyrin)(Cl) in 70 mL of C_6H_6 or CH_2Cl_2 was added 25 mL of a saturated aqueous solution of $S_2O_4Na_2$. The reaction mixture was stirred, under argon, for 0.25 h during which time the solution changed from brown to red. An electronic spectrum of a sample (diluted in C_6H_6) was recorded to confirm the reduction of Fe^{III}(porphyrin)(Cl) to Fe^{II}-(porphyrin). The organic layer was added to 1.2 mmol of complex **1** previously deaerated by bubbling argon and stirred for 1 h at 50 °C. The red color turned progressively green. After solvent evaporation, the crude product was purified by a column chromatography (SiO_2, CH_2Cl_2/CH_3COCH_3$, 8:2) and crystallized from a CH_2Cl_2–pentane mixture. Complexes **5** were obtained as green crystals in excellent yields (>95%).

(2) From Complexes 3. To a deaerated solution of 0.1 mmol of complex **3a**, **3b**, or **3c** in 30 mL of C_6H_6 was added 10 mL of a saturated aqueous solution of $Na_2S_2O_4$. The reaction mixture immediately turned light green. The organic layer was added to 0.4 mmol of compound **1** previously deaerated, and the color immediately turned dark green. The electronic spectrum of a sample diluted in C_6H_6 showed the characteristic spectra of the corresponding complexes **5**. After a similar workup as in method 1, complexes **5a**, **5b**, or **5c** were each obtained in quantitative yield. Complex **5a** Fe(TPP)(C$_8$H$_{10}$O$_2$)$_2$·2H$_2$O: Anal. Calcd (found) for $C_{60}H_{52}N_4FeO_6$: C, 73.43 (73.54); H, 5.31 (5.21); N, 5.71 (5.72). Complex **5b** Fe(TpClPP)(C$_8$H$_{10}$O$_2$)$_2$·2H$_2$O: Anal. Calcd (found) for $C_{60}H_{48}N_4FeCl_4O_6$: C, 64.40 (64.66); H, 4.29 (4.49); N, 5.01 (5.05); Cl,

(36) Lexa, D.; Saveant, J. M.; Zieckler, J. *J. Am. Chem. Soc.* **1977**, *99*, 2786–2790.

(37) Frenz, B. A. *The Enraf-Nonius C4D4-SPD in Computing in Crystallography*; Schenk, H., Olthof-Hazekamp, R., Van Koningsveld, H., Bassi, G. C., Eds.; Delft University Press: 1978; pp 64–71.

(38) Lehmann, M. S.; Larsen, F. K. *Acta Crystallogr., Sect. A: Cryst. Phys., Diffr., Theor. Gen. Crystallogr.* **1974**, *A30*, 580–584.

(39) Busing, W. R.; Levy, H. A. *Acta Crystallogr.* **1957**, *10*, 180–182.

(40) Cromer, D. T.; Waber, J. T. *International Tables for X-ray Crystallography*; Kynoch: Birmingham, England, **1974**; p 4, Table 2.2b.

(41) Cromer, D. T.; Waber, J. T. *International Tables for X-ray Crystallography*; Kynoch: Birmingham, England, **1974**, p 4, Table 2.3.1.

12.70 (12.96). Complexes **5c** Fe(TTP)(C₈H₁₀O₂)₂·2H₂O: Anal. Calcd (found) for C₆₄H₆₀N₄FeO₆: 74.12 (74.92); H, 5.83 (5.70); N, 5.40 (5.51).

Supplementary Material Available: Concerning the X-ray structure of complex **5a**: Table V, thermal parameters for nonhydrogen atoms; Table VI, positional parameters for hydrogen atoms; Table VIII, bond distances; Table IX, bond angles; Table X, least-squares mean planes of interest (13 pages); Table VII, calculated and observed structure factor amplitudes (×10) for all observed reflections (14 pages). Ordering information is given on any current masthead page.

A New Inorganic Ring System: Planar Fe₃(μ₂-SR)₃ in [Fe₃(SR)₃X₆]³⁻—Synthesis, Structures, and Solution Conformation and Equilibrium

M. A. Whitener,[1a] **J. K. Bashkin,**[1a,b] **K. S. Hagen,**[1a] **J.-J. Girerd,**[1c] **E. Gamp,**[1d]
N. Edelstein,[1d] **and R. H. Holm***[1a]

*Contribution from the Department of Chemistry, Harvard University,
Cambridge, Massachusetts 02138, the Laboratoire de Spectrochimie des Élements de Transition,
ERA CNRS 672, Université de Paris-Sud, F-91405 Orsay, France, and the Materials and
Molecular Research Division, Lawrence Berkeley Laboratory, Berkeley, California 94720.
Received December 2, 1985*

Abstract: Anaerobic reaction of equimolar FeX₂ and RS⁻ in acetonitrile affords the trinuclear complexes [Fe₃(SR)₃X₆]³⁻ (with X = Cl and R = Ph (**4a**), *p*-tolyl (**4b**), 2,6-Me₂C₆H₃ (**4d**), and X = Br, R = Ph (**4c**)) isolated as Et₄N⁺ salts. These species constitute the fourth known type of discrete Fe(II) thiolates, the others being [Fe(SR)₄]²⁻, [Fe₂(SR)₆]²⁻, and [Fe₄(SR)₁₀]²⁻. The following crystallographic results were obtained (crystal system; space group; cell parameters; Z; unique data (*I* > 3σ(*I*)); *R* (%)). (Et₄N)₃ (**4a**): monoclinic; C2/c; a = 24.500 (6) Å, b = 13.488 (3) Å, c = 18.217 (5) Å, β = 110.68 (2)°; 4; 2679; 4.9. (Et₄N)₃ (**4d**)·3MeCN: monoclinic: P2₁/n; a = 15.07 (1) Å, b = 22.38 (3) Å, c = 20.46 (3) Å, β = 91.5 (1)°; 4; 3311; 9.7. (Et₄N)₃ (**4c**)·MeCN: hexagonal; P6̄2c; a = b = 13.970 (4) Å, c = 18.274 (3) Å; 2; 890; 5.7. The reaction system FeBr₂ + NaSCH₂Ph in acetonitrile yields a different type of compound with the composition (Et₄N)₂[Fe₄(SCH₂Ph)₆Br₄] (**5**): triclinic; P1̄; a = 12.874 (2) Å, b = 13.949 (3) Å, c = 43.272 (8) Å, α = 94.85 (2)°, β = 94.07 (2)°, γ = 114.98 (1)°; 4; 7402; 6.7. Anions of type **4** contain a new type of inorganic ring system, Fe₃(μ₂-SR)₃, distinguished by its nearly or exactly planar conformation and unusually large Fe–S–Fe angles of ~140°, the largest values observed for this angle type. The phenyl groups in **4a** and **4c** (which has imposed C₃ₕ symmetry) are coplanar with the Fe₃S₃ rings. In **4d** these groups are rotated by ~90° owing to the steric effects of the methyl groups. Distorted tetrahedral coordination at each Fe(II) atom is completed by two halide ligands. The planar structure is to be contrasted with the chair-type conformation of the rings in **5** and other species with adamantane-like stereochemistry. Ring conformations influence the extent of antiferromagnetic interactions in the solid state. Magnetic susceptibility data of planar **4a** are fit well by two –*J* values at 19–22 cm⁻¹. For [Fe₄(SR)₁₀]²⁻, containing adamantane-like Fe₄(μ₂-SR)₆ cages with Fe₃(μ₂-SR)₃ rings in the chair conformation, best fits of the magnetic data give one –*J* value at 32 or 36 cm⁻¹ and one or two others at 42–66 cm⁻¹ depending on the coupling symmetry. MO calculations at the extended Hückel level on [Fe₃(SH)₃Cl₆]³⁻ suggest that the inherently stable conformation of the ring is planar. This structure is set in large measure by the stereochemical preference of the S–Fe–S angle and by transannular nonbonded repulsions. The decrease in Cl···Cl distances from 6.6 to 3.9 Å in changing from the planar to the chair conformation emphasizes the latter effect. In acetonitrile the equilibrium 2[Fe₃(SR)₃X₆]³⁻ ⇌ [Fe₄(SR)₆X₄]²⁻ + 2[FeCl₄]²⁻ has been approached in both directions and is shifted to the left with decreasing temperature. At ≤240 K the formation of [Fe₃(SR)₃X₆]³⁻ is essentially complete. In this temperature range the magnetic moment per Fe atom (μ_Fe) is 4.1–4.2 μ_B for **4a** in solution and as its crystalline Et₄N⁺ salt. This excellent agreement establishes a planar ring conformation in solution. Thus the results of three crystal structures, MO calculations, and solution and solid state magnetic measurements collectively demonstrate that the near or exact planarity of the Fe₃S₃ cycles in [Fe₃(SR)₃X₆]³⁻ is an intrinsic property.

Previous investigations in this laboratory have demonstrated reactions 1–4 in Figure 1, affording the complexes [Fe(SR)₄]²⁻ (**1**), [Fe₂(SR)₆]²⁻ (**2**), [Fe₄(SR)₁₀]²⁻ (**3**), and [Fe₃(SR)₃Cl₆]³⁻ (**4**).[2-7] Several additional examples of **2** have been prepared by

others.[8] The set **1–4**, containing species of varying nuclearity based on tetrahedral Fe(II) coordination, has a number of significant aspects. In reactions with elemental sulfur, **1–3** are precursors to a variety of Fe–S–SR clusters.[2,4,5,9] These same complexes serve as structural prototypes of related thiolate complexes formed by M(II) ions with tetrahedral stereochemical preference. An expanding number of such complexes have been prepared and structurally characterized.[10,11] Complex **4a** (R =

(1) (a) Harvard University. (b) NIH Postdoctoral Fellow, 1984–1985. (c) University of Paris. (d) Lawrence Berkeley Laboratory.
(2) Hagen, K. S.; Reynolds, J. G.; Holm, R. H. *J. Am. Chem. Soc.* **1981**, *103*, 4054.
(3) Hagen, K. S.; Stephan, D. W.; Holm, R. H. *Inorg. Chem.* **1982**, *21*, 3928.
(4) Hagen, K. S.; Holm, R. H. *J. Am. Chem. Soc.* **1982**, *104*, 5496.
(5) Hagen, K. S.; Watson, A. D.; Holm. R. H. *J. Am. Chem. Soc.* **1983**, *105*, 3905.
(6) Hagen, K. S.; Holm, R. H. *Inorg. Chem.* **1984**, *23*, 418.

(7) Holm, R. H.; Hagen, K. S., Watson, A. D. In *Chemistry for the Future*; Grünewald, H., Ed.; New York: Pergamon Press, 1984; pp 115–124.
(8) Henkel, G.; Tremel, W.; Krebs, B. *Angew. Chem., Int. Ed. Engl.* **1983**, *22*, 319.
(9) Kurtz, D. M., Jr.; Stevens, W. C. *J. Am. Chem. Soc.* **1984**, *106*, 1523.